

# Nonlinear Fiber Optics

FOURTH EDITION



Govind P. Agrawal

# **Nonlinear Fiber Optics**

*Fourth Edition*

"This page intentionally left blank"

# Nonlinear Fiber Optics

*Fourth Edition*

**GOVIND P. AGRAWAL**

*The Institute of Optics*

*University of Rochester*

*Rochester, New York*



**ELSEVIER**

AMSTERDAM • BOSTON • HEIDELBERG • LONDON  
NEW YORK • OXFORD • PARIS • SAN DIEGO  
SAN FRANCISCO • SINGAPORE • SYDNEY • TOKYO

Academic Press is an imprint of Elsevier



**ACADEMIC  
PRESS**

Academic Press is an imprint of Elsevier  
30 Corporate Drive, Suite 400, Burlington, MA 01803, USA  
525 B Street, Suite 1900, San Diego, California 92101-4495, USA  
84 Theobald's Road, London WC1X 8RR, UK

This book is printed on acid-free paper. ©

Copyright © 2007 Elsevier Inc. All rights reserved.

No part of this publication may be reproduced or transmitted in any form or by any means, electronic or mechanical, including photocopy, recording, or any information storage and retrieval system, without permission in writing from the publisher.

Requests for permission to make copies of any part of the work should be mailed to: Permissions Department, Harcourt, Inc., 6277 Sea Harbor Drive, Orlando, Florida 32887-6777.

Permissions may be sought directly from Elsevier's Science & Technology Rights Department in Oxford, UK: phone: (+44) 1865 843830, fax: (+44) 1865 853333, E-mail: [permissions@elsevier.com](mailto:permissions@elsevier.com). You may also complete your request on-line via the Elsevier homepage (<http://elsevier.com>), by selecting "Support & Contact" then "Copyright and Permission" and then "Obtaining Permissions."

#### **Library of Congress Cataloging-in-Publication Data**

Application submitted.

#### **British Library Cataloguing-in-Publication Data**

A catalogue record for this book is available from the British Library.

ISBN 13: 978-0-12-369516-1

ISBN 10: 0-12-369516-3

For information on all Academic Press publications  
visit our Web site at [www.books.elsevier.com](http://www.books.elsevier.com)

Printed in the United States of America

06 07 08 09 10 9 8 7 6 5 4 3 2 1

Working together to grow  
libraries in developing countries

[www.elsevier.com](http://www.elsevier.com) | [www.bookaid.org](http://www.bookaid.org) | [www.sabre.org](http://www.sabre.org)

**ELSEVIER**

**BOOK AID**  
International

**Sabre Foundation**

*In the memory of my mother and  
for Anne, Sipra, Caroline, and Claire*

"This page intentionally left blank"

# Contents

<b>Preface</b>	<b>xv</b>
<b>1 Introduction</b>	<b>1</b>
1.1 Historical Perspective . . . . .	1
1.2 Fiber Characteristics . . . . .	3
1.2.1 Material and Fabrication . . . . .	4
1.2.2 Fiber Losses . . . . .	5
1.2.3 Chromatic Dispersion . . . . .	6
1.2.4 Polarization-Mode Dispersion . . . . .	11
1.3 Fiber Nonlinearities . . . . .	13
1.3.1 Nonlinear Refraction . . . . .	14
1.3.2 Stimulated Inelastic Scattering . . . . .	15
1.3.3 Importance of Nonlinear Effects . . . . .	17
1.4 Overview . . . . .	18
Problems . . . . .	20
References . . . . .	21
<b>2 Pulse Propagation in Fibers</b>	<b>25</b>
2.1 Maxwell's Equations . . . . .	25
2.2 Fiber Modes . . . . .	27
2.2.1 Eigenvalue Equation . . . . .	28
2.2.2 Single-Mode Condition . . . . .	29
2.2.3 Characteristics of the Fundamental Mode . . . . .	30
2.3 Pulse-Propagation Equation . . . . .	31
2.3.1 Nonlinear Pulse Propagation . . . . .	32
2.3.2 Higher-Order Nonlinear Effects . . . . .	36
2.4 Numerical Methods . . . . .	41
2.4.1 Split-Step Fourier Method . . . . .	41
2.4.2 Finite-Difference Methods . . . . .	45
Problems . . . . .	46
References . . . . .	47



<b>3</b>	<b>Group-Velocity Dispersion</b>	<b>51</b>
3.1	Different Propagation Regimes . . . . .	51
3.2	Dispersion-Induced Pulse Broadening . . . . .	53
3.2.1	Gaussian Pulses . . . . .	54
3.2.2	Chirped Gaussian Pulses . . . . .	56
3.2.3	Hyperbolic Secant Pulses . . . . .	58
3.2.4	Super-Gaussian Pulses . . . . .	58
3.2.5	Experimental Results . . . . .	61
3.3	Third-Order Dispersion . . . . .	62
3.3.1	Evolution of Chirped Gaussian Pulses . . . . .	63
3.3.2	Broadening Factor . . . . .	65
3.3.3	Arbitrary-Shape Pulses . . . . .	67
3.3.4	Ultrashort-Pulse Measurements . . . . .	69
3.4	Dispersion Management . . . . .	71
3.4.1	GVD-Induced Limitations . . . . .	71
3.4.2	Dispersion Compensation . . . . .	73
3.4.3	Compensation of Third-Order Dispersion . . . . .	74
	Problems . . . . .	76
	References . . . . .	77
<b>4</b>	<b>Self-Phase Modulation</b>	<b>79</b>
4.1	SPM-Induced Spectral Changes . . . . .	79
4.1.1	Nonlinear Phase Shift . . . . .	80
4.1.2	Changes in Pulse Spectra . . . . .	82
4.1.3	Effect of Pulse Shape and Initial Chirp . . . . .	85
4.1.4	Effect of Partial Coherence . . . . .	87
4.2	Effect of Group-Velocity Dispersion . . . . .	89
4.2.1	Pulse Evolution . . . . .	90
4.2.2	Broadening Factor . . . . .	91
4.2.3	Optical Wave Breaking . . . . .	94
4.2.4	Experimental Results . . . . .	97
4.2.5	Effect of Third-Order Dispersion . . . . .	98
4.2.6	SPM Effects in Fiber Amplifiers . . . . .	100
4.3	Semianalytic Techniques . . . . .	102
4.3.1	Moment Method . . . . .	102
4.3.2	Variational Method . . . . .	103
4.3.3	Specific Analytic Solutions . . . . .	104
4.4	Higher-Order Nonlinear Effects . . . . .	106
4.4.1	Self-Steepening . . . . .	107
4.4.2	Effect of GVD on Optical Shocks . . . . .	109
4.4.3	Intrapulse Raman Scattering . . . . .	111
	Problems . . . . .	114
	References . . . . .	116

<b>5</b>	<b>Optical Solitons</b>	<b>120</b>
5.1	Modulation Instability . . . . .	120
5.1.1	Linear Stability Analysis . . . . .	121
5.1.2	Gain Spectrum . . . . .	122
5.1.3	Experimental Results . . . . .	124
5.1.4	Ultrashort Pulse Generation . . . . .	125
5.1.5	Impact on Lightwave Systems . . . . .	127
5.2	Fiber Solitons . . . . .	129
5.2.1	Inverse Scattering Method . . . . .	130
5.2.2	Fundamental Soliton . . . . .	132
5.2.3	Higher-Order Solitons . . . . .	134
5.2.4	Experimental Confirmation . . . . .	136
5.2.5	Soliton Stability . . . . .	137
5.3	Other Types of Solitons . . . . .	140
5.3.1	Dark Solitons . . . . .	140
5.3.2	Dispersion-Managed Solitons . . . . .	144
5.3.3	Bistable Solitons . . . . .	144
5.4	Perturbation of Solitons . . . . .	146
5.4.1	Perturbation Methods . . . . .	146
5.4.2	Fiber Losses . . . . .	147
5.4.3	Soliton Amplification . . . . .	149
5.4.4	Soliton Interaction . . . . .	152
5.5	Higher-Order Effects . . . . .	156
5.5.1	Moment Equations for Pulse Parameters . . . . .	156
5.5.2	Third-Order Dispersion . . . . .	158
5.5.3	Self-Steepening . . . . .	160
5.5.4	Intrapulse Raman Scattering . . . . .	162
5.5.5	Propagation of Femtosecond Pulses . . . . .	167
	Problems . . . . .	169
	References . . . . .	170
<b>6</b>	<b>Polarization Effects</b>	<b>177</b>
6.1	Nonlinear Birefringence . . . . .	177
6.1.1	Origin of Nonlinear Birefringence . . . . .	178
6.1.2	Coupled-Mode Equations . . . . .	180
6.1.3	Elliptically Birefringent Fibers . . . . .	181
6.2	Nonlinear Phase Shift . . . . .	182
6.2.1	Nondispersive XPM . . . . .	182
6.2.2	Optical Kerr Effect . . . . .	183
6.2.3	Pulse Shaping . . . . .	187
6.3	Evolution of Polarization State . . . . .	189
6.3.1	Analytic Solution . . . . .	189
6.3.2	Poincaré-Sphere Representation . . . . .	191
6.3.3	Polarization Instability . . . . .	194
6.3.4	Polarization Chaos . . . . .	196
6.4	Vector Modulation Instability . . . . .	197

6.4.1	Low-Birefringence Fibers . . . . .	197
6.4.2	High-Birefringence Fibers . . . . .	200
6.4.3	Isotropic Fibers . . . . .	202
6.4.4	Experimental Results . . . . .	203
6.5	Birefringence and Solitons . . . . .	206
6.5.1	Low-Birefringence Fibers . . . . .	206
6.5.2	High-Birefringence Fibers . . . . .	207
6.5.3	Soliton-Dragging Logic Gates . . . . .	211
6.5.4	Vector Solitons . . . . .	212
6.6	Random Birefringence . . . . .	213
6.6.1	Polarization-Mode Dispersion . . . . .	214
6.6.2	Vector Form of the NLS Equation . . . . .	215
6.6.3	Effects of PMD on Solitons . . . . .	216
	Problems . . . . .	220
	References . . . . .	221
<b>7</b>	<b>Cross-Phase Modulation</b>	<b>226</b>
7.1	XPM-Induced Nonlinear Coupling . . . . .	227
7.1.1	Nonlinear Refractive Index . . . . .	227
7.1.2	Coupled NLS Equations . . . . .	228
7.2	XPM-Induced Modulation Instability . . . . .	229
7.2.1	Linear Stability Analysis . . . . .	229
7.2.2	Experimental Results . . . . .	232
7.3	XPM-Paired Solitons . . . . .	233
7.3.1	Bright–Dark Soliton Pair . . . . .	233
7.3.2	Bright–Gray Soliton Pair . . . . .	234
7.3.3	Periodic Solutions . . . . .	235
7.3.4	Multiple Coupled NLS Equations . . . . .	237
7.4	Spectral and Temporal Effects . . . . .	238
7.4.1	Asymmetric Spectral Broadening . . . . .	239
7.4.2	Asymmetric Temporal Changes . . . . .	244
7.4.3	Higher-Order Nonlinear Effects . . . . .	247
7.5	Applications of XPM . . . . .	248
7.5.1	XPM-Induced Pulse Compression . . . . .	248
7.5.2	XPM-Induced Optical Switching . . . . .	251
7.5.3	XPM-Induced Nonreciprocity . . . . .	252
7.6	Polarization Effects . . . . .	254
7.6.1	Vector Theory of XPM . . . . .	254
7.6.2	Polarization Evolution . . . . .	255
7.6.3	Polarization-Dependent Spectral Broadening . . . . .	257
7.6.4	Pulse Trapping and Compression . . . . .	260
7.6.5	XPM-Induced Wave Breaking . . . . .	262
7.7	XPM Effects in Birefringent Fibers . . . . .	264
7.7.1	Fibers with Low Birefringence . . . . .	264
7.7.2	Fibers with High Birefringence . . . . .	267
	Problems . . . . .	268

References . . . . .	270
<b>8 Stimulated Raman Scattering</b>	<b>274</b>
8.1 Basic Concepts . . . . .	274
8.1.1 Raman-Gain Spectrum . . . . .	275
8.1.2 Raman Threshold . . . . .	276
8.1.3 Coupled Amplitude Equations . . . . .	279
8.1.4 Effect of Four-Wave Mixing . . . . .	281
8.2 Quasi-Continuous SRS . . . . .	283
8.2.1 Single-Pass Raman Generation . . . . .	283
8.2.2 Raman Fiber Lasers . . . . .	285
8.2.3 Raman Fiber Amplifiers . . . . .	288
8.2.4 Raman-Induced Crosstalk . . . . .	292
8.3 SRS with Short Pump Pulses . . . . .	294
8.3.1 Pulse-Propagation Equations . . . . .	294
8.3.2 Nondispersive Case . . . . .	295
8.3.3 Effects of GVD . . . . .	297
8.3.4 Experimental Results . . . . .	300
8.3.5 Synchronously Pumped Raman Lasers . . . . .	304
8.3.6 Short-Pulse Raman Amplification . . . . .	305
8.4 Soliton Effects . . . . .	306
8.4.1 Raman Solitons . . . . .	306
8.4.2 Raman Soliton Lasers . . . . .	311
8.4.3 Soliton-Effect Pulse Compression . . . . .	313
8.5 Polarization Effects . . . . .	315
8.5.1 Vector Theory of Raman Amplification . . . . .	315
8.5.2 PMD Effects on Raman Amplification . . . . .	319
Problems . . . . .	321
References . . . . .	322
<b>9 Stimulated Brillouin Scattering</b>	<b>329</b>
9.1 Basic Concepts . . . . .	329
9.1.1 Physical Process . . . . .	330
9.1.2 Brillouin-Gain Spectrum . . . . .	330
9.2 Quasi-CW SBS . . . . .	333
9.2.1 Brillouin Threshold . . . . .	333
9.2.2 Polarization Effects . . . . .	334
9.2.3 Techniques for Controlling the SBS Threshold . . . . .	335
9.2.4 Experimental Results . . . . .	338
9.3 Brillouin Fiber Amplifiers . . . . .	340
9.3.1 Gain Saturation . . . . .	341
9.3.2 Amplifier Design and Applications . . . . .	342
9.4 SBS Dynamics . . . . .	344
9.4.1 Coupled Amplitude Equations . . . . .	345
9.4.2 SBS with Q-Switched Pulses . . . . .	346
9.4.3 SBS-Induced Index Changes . . . . .	350

9.4.4	Relaxation Oscillations . . . . .	352
9.4.5	Modulation Instability and Chaos . . . . .	354
9.5	Brillouin Fiber Lasers . . . . .	356
9.5.1	CW Operation . . . . .	356
9.5.2	Pulsed Operation . . . . .	360
Problems	. . . . .	362
References	. . . . .	363
<b>10</b>	<b>Four-Wave Mixing</b>	<b>368</b>
10.1	Origin of Four-Wave Mixing . . . . .	368
10.2	Theory of Four-Wave Mixing . . . . .	370
10.2.1	Coupled Amplitude Equations . . . . .	371
10.2.2	Approximate Solution . . . . .	371
10.2.3	Effect of Phase Matching . . . . .	373
10.2.4	Ultrafast Four-Wave Mixing . . . . .	374
10.3	Phase-Matching Techniques . . . . .	376
10.3.1	Physical Mechanisms . . . . .	376
10.3.2	Phase Matching in Multimode Fibers . . . . .	377
10.3.3	Phase Matching in Single-Mode Fibers . . . . .	380
10.3.4	Phase Matching in Birefringent Fibers . . . . .	383
10.4	Parametric Amplification . . . . .	387
10.4.1	Review of Early Work . . . . .	387
10.4.2	Gain Spectrum and Its Bandwidth . . . . .	389
10.4.3	Single-Pump Configuration . . . . .	391
10.4.4	Dual-Pump Configuration . . . . .	394
10.4.5	Effects of Pump Depletion . . . . .	399
10.5	Polarization Effects . . . . .	401
10.5.1	Vector Theory of Four-Wave Mixing . . . . .	401
10.5.2	Polarization Dependence of Parametric Gain . . . . .	403
10.5.3	Linearly and Circularly Polarized Pumps . . . . .	405
10.5.4	Effect of Residual Fiber Birefringence . . . . .	408
10.6	Applications of Four-Wave Mixing . . . . .	411
10.6.1	Parametric Oscillators . . . . .	412
10.6.2	Ultrafast Signal Processing . . . . .	413
10.6.3	Quantum Noise and Correlation . . . . .	415
Problems	. . . . .	417
References	. . . . .	418
<b>11</b>	<b>Highly Nonlinear Fibers</b>	<b>424</b>
11.1	Nonlinear Parameter . . . . .	424
11.1.1	Units and Values of $n_2$ . . . . .	425
11.1.2	SPM-Based Techniques . . . . .	426
11.1.3	XPM-Based Technique . . . . .	429
11.1.4	FWM-Based Technique . . . . .	430
11.1.5	Variations in $n_2$ Values . . . . .	431
11.2	Fibers with Silica Cladding . . . . .	434

11.3 Tapered Fibers with Air Cladding . . . . .	436
11.4 Microstructured Fibers . . . . .	440
11.5 Non-Silica Fibers . . . . .	444
Problems . . . . .	448
References . . . . .	449
<b>12 Novel Nonlinear Phenomena</b>	<b>453</b>
12.1 Intrapulse Raman Scattering . . . . .	453
12.1.1 Enhanced RIFS and Wavelength Tuning . . . . .	454
12.1.2 Nonsolitonic Radiation . . . . .	457
12.1.3 Effects of Birefringence . . . . .	459
12.1.4 Suppression of Raman-Induced Frequency Shifts . . . . .	461
12.2 Four-Wave Mixing . . . . .	464
12.2.1 FWM in Highly Nonlinear Fibers . . . . .	464
12.2.2 Effects of Fiber Birefringence . . . . .	467
12.3 Supercontinuum Generation . . . . .	469
12.3.1 Pumping with Picosecond Pulses . . . . .	470
12.3.2 Continuous-Wave Pumping . . . . .	474
12.3.3 Pumping with Femtosecond Pulses . . . . .	475
12.4 Temporal and Spectral Evolution . . . . .	477
12.4.1 Numerical Modeling of Supercontinuum . . . . .	477
12.4.2 Soliton Fission and Nonsolitonic Radiation . . . . .	480
12.4.3 Effects of Cross-Phase Modulation . . . . .	484
12.4.4 Polarization Effects . . . . .	488
12.4.5 Coherence Properties of a Supercontinuum . . . . .	492
12.5 Harmonic Generation . . . . .	495
12.5.1 Second-Harmonic Generation . . . . .	495
12.5.2 Third-Harmonic Generation . . . . .	502
Problems . . . . .	506
References . . . . .	507
<b>A System of Units</b>	<b>514</b>
<b>B Numerical Code for the NLS Equation</b>	<b>516</b>
<b>C List of Acronyms</b>	<b>519</b>
<b>Index</b>	<b>521</b>

"This page intentionally left blank"

# Preface

Since the publication of the first edition of this book in 1989, the field of *nonlinear fiber optics* has remained an active area of research and has thus continued to grow at a rapid pace. During the 1990s, a major factor behind such a sustained growth was the advent of fiber amplifiers and lasers, made by doping silica fibers with rare-earth materials such as erbium and ytterbium. Erbium-doped fiber amplifiers revolutionized the design of fiber-optic communication systems, including those making use of optical solitons, whose very existence stems from the presence of nonlinear effects in optical fibers. Optical amplifiers permit propagation of lightwave signals over thousands of kilometers as they can compensate for all losses encountered by the signal in the optical domain. At the same time, fiber amplifiers enable the use of massive wavelength-division multiplexing, a technique that led by 1999 to the development of lightwave systems with capacities exceeding 1 Tb/s. Nonlinear fiber optics plays an important role in the design of such high-capacity lightwave systems. In fact, an understanding of various nonlinear effects occurring inside optical fibers is almost a prerequisite for a lightwave-system designer.

Starting around 2000, a new development occurred in the field of *nonlinear fiber optics* that changed the focus of research and has led to a number of advances and novel applications in recent years. Several kinds of new fibers, classified as highly nonlinear fibers, have been developed. They are referred to with names such as microstructured fibers, holey fibers, or photonic crystal fibers, and share the common property that a relatively narrow core is surrounded by a cladding containing a large number of air holes. The nonlinear effects are enhanced dramatically in such fibers to the extent that they can be observed even when the fiber is only a few centimeters long. Their dispersive properties are also quite different compared with those of conventional fibers developed for telecommunication applications. Because of these changes, microstructured fibers exhibit a variety of novel nonlinear effects that are finding applications in fields as diverse as optical coherence tomography and high-precision frequency metrology.

The fourth edition is intended to bring the book up-to-date so that it remains a unique source of comprehensive coverage on the subject of nonlinear fiber optics. It retains most of the material that appeared in the third edition. However, an attempt was made to include recent research results on all topics relevant to the field of nonlinear fiber optics. Such an ambitious objective has increased the size of the book considerably. Two new chapters, Chapters 11 and 12, have been added to cover the recent research advances. Chapter 11 describes the properties of highly nonlinear fibers, and the novel nonlinear effects that have been observed since 2000 in such fibers are cov-



ered in Chapter 12. Although all other chapters have been updated, Chapters 8 to 10 required major additions because of the recent advances in the research areas covered by them. For example, polarization issues have become increasingly more important for stimulated Raman scattering and four-wave mixing, and thus they are discussed in detail in Chapters 8 and 10. It is important that students learn about such polarization effects in a course devoted to nonlinear fiber optics.

The potential readership is likely to consist of senior undergraduate students, graduate students enrolled in the M.S. and Ph.D. degree programs, engineers and technicians involved with the fiber-optics industry, and scientists working in the fields of fiber optics and optical communications. This revised edition should continue to be a useful text for graduate and senior-level courses dealing with nonlinear optics, fiber optics, or optical communications that are designed to provide mastery of the fundamental aspects. Some universities may even opt to offer a high-level graduate course devoted to solely nonlinear fiber optics. The problems provided at the end of each chapter should be useful to instructors of such a course.

Many individuals have contributed, either directly or indirectly, to the completion of the third edition. I am thankful to all of them, especially to my graduate students whose curiosity and involvement led to several improvements. Several of my colleagues have helped me in preparing the fourth edition. I especially thank F. Omenetto, Q. Lin, and F. Yaman for reading drafts of selected chapters and for making helpful suggestions. I am grateful to many readers for their occasional feedback. Last, but not least, I thank my wife, Anne, and my daughters, Sipra, Caroline, and Claire, for understanding why I needed to spend many weekends on the book instead of spending time with them.

Govind P. Agrawal  
Rochester, New York  
July 2006

"This page intentionally left blank"

# Chapter 1

## Introduction

This introductory chapter is intended to provide an overview of the fiber characteristics that are important for understanding the nonlinear effects discussed in later chapters. Section 1.1 provides a historical perspective on the progress in the field of fiber optics. Section 1.2 discusses various fiber properties such as optical loss, chromatic dispersion, and birefringence. Particular attention is paid to chromatic dispersion because of its importance in the study of nonlinear effects probed by using ultrashort optical pulses. Section 1.3 introduces various nonlinear effects resulting from the intensity dependence of the refractive index and stimulated inelastic scattering. Among the nonlinear effects that have been studied extensively using optical fibers as a nonlinear medium are self-phase modulation, cross-phase modulation, four-wave mixing, stimulated Raman scattering, and stimulated Brillouin scattering. Each of these effects is considered in detail in separate chapters. Section 1.4 gives an overview of how this book is organized for discussing such a wide variety of nonlinear effects in optical fibers.

### 1.1 Historical Perspective

Total internal reflection—the basic phenomenon responsible for guiding of light in optical fibers—is known from the nineteenth century. The reader is referred to a 1999 book for the interesting history behind the discovery of this phenomenon [1]. Although uncladded glass fibers were fabricated in the 1920s [2]–[4], the field of fiber optics was not born until the 1950s when the use of a cladding layer led to considerable improvement in the fiber characteristics [5]–[8]. The idea that optical fibers would benefit from a dielectric cladding was not obvious and has a remarkable history [1].

The field of fiber optics developed rapidly during the 1960s, mainly for the purpose of image transmission through a bundle of glass fibers [9]. These early fibers were extremely lossy (loss  $>1000$  dB/km) from the modern standard. However, the situation changed drastically in 1970 when, following an earlier suggestion [10], losses of silica fibers were reduced to below 20 dB/km [11]. Further progress in fabrication technology [12] resulted by 1979 in a loss of only 0.2 dB/km in the 1.55- $\mu\text{m}$  wave-

length region [13], a loss level limited mainly by the fundamental process of Rayleigh scattering.

The availability of low-loss silica fibers led not only to a revolution in the field of optical fiber communications [14]–[17] but also to the advent of the new field of nonlinear fiber optics. Stimulated Raman- and Brillouin-scattering processes in optical fibers were studied as early as 1972 [18]–[20]. This work stimulated the study of other nonlinear phenomena such as optically induced birefringence, parametric four-wave mixing, and self-phase modulation [21]–[25]. An important contribution was made in 1973 when it was suggested that optical fibers can support soliton-like pulses as a result of an interplay between the dispersive and nonlinear effects [26]. Optical solitons were observed in a 1980 experiment [27] and led to a number of advances during the 1980s in the generation and control of ultrashort optical pulses [28]–[32]. The decade of the 1980s also saw the development of pulse-compression and optical-switching techniques that exploited the nonlinear effects in fibers [33]–[40]. Pulses as short as 6 fs were generated by 1987 [41]. The first edition of this book covered the progress made during the 1980s [42]–[47].

The field of nonlinear fiber optics continued to grow during the decade of the 1990s. A new dimension was added when optical fibers were doped with rare-earth elements and used to make amplifiers and lasers. Although fiber amplifiers were made as early as 1964 [48], it was only after 1987 that their development accelerated [49]. Erbium-doped fiber amplifiers attracted the most attention because they operate in the wavelength region near  $1.55\text{ }\mu\text{m}$  and are thus useful for fiber-optic lightwave systems [50]. Their use led to a virtual revolution in the design of multichannel lightwave systems [14]–[17]. After 2000, two nonlinear effects occurring inside optical fibers, namely stimulated Raman scattering and four-wave mixing, were employed to develop new types of fiber-optic amplifiers. Such amplifiers do not require doped fibers and can operate in any spectral region. Indeed, the use of Raman amplification has become quite common in modern telecommunication systems [51]. Fiber-optic parametric amplifiers based on four-wave mixing are also attractive because of their potential for ultrafast signal processing [52].

The advent of fiber amplifiers also fueled research on optical solitons and led eventually to new types of solitons such as dispersion-managed solitons and dissipative solitons [53]–[56]. In another development, fiber gratings, first made in 1978 [57], were developed during the 1990s to the point that they became an integral part of lightwave technology [58]. Starting in 1996, new types of fibers, known under names such as photonic crystal fibers, holey fibers, microstructure fibers, and tapered fibers, were developed [59]–[63]. Structural changes in such fibers affect their dispersive as well as nonlinear properties. In particular, the wavelength at which the group-velocity dispersion vanishes shifts toward the visible region. Some fibers exhibit two such wavelengths such that dispersion is anomalous in the visible and near-infrared regions. At the same time, the nonlinear effects are enhanced considerably because of a relatively small core size. This combination leads to supercontinuum generation, a phenomenon in which the optical spectrum of ultrashort pulses is broadened by a factor of more than 200 over a length of only 1 m or less [64]–[66]. With these developments, the field of nonlinear fiber optics has grown considerably after 2000 and is expected to continue to do so in the near future.

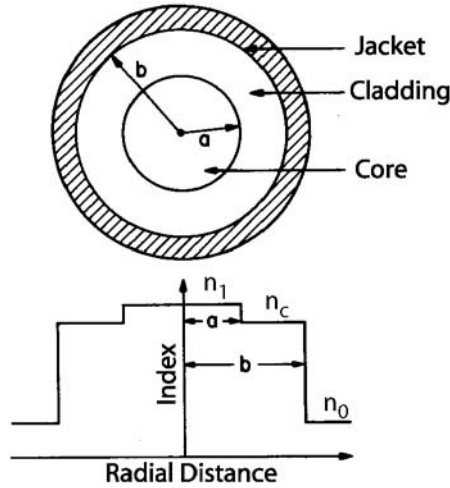


**Figure 1.1:** Schematic illustration of the cross section and the refractive-index profile of a step-index fiber.

## 1.2 Fiber Characteristics

In its simplest form, an optical fiber consists of a central glass core surrounded by a cladding layer whose refractive index  $n_c$  is slightly lower than the core index  $n_1$ . Such fibers are generally referred to as *step-index fibers* to distinguish them from *graded-index fibers* in which the refractive index of the core decreases gradually from center to core boundary [67]–[69]. Figure 1.1 shows schematically the cross section and refractive-index profile of a step-index fiber. Two parameters that characterize an optical fiber are the relative core–cladding index difference

$$\Delta = \frac{n_1 - n_c}{n_1} \quad (1.2.1)$$

and the so-called  $V$  parameter defined as

$$V = k_0 a (n_1^2 - n_c^2)^{1/2}, \quad (1.2.2)$$

where  $k_0 = 2\pi/\lambda$ ,  $a$  is the core radius, and  $\lambda$  is the wavelength of light.

The  $V$  parameter determines the number of modes supported by the fiber. Fiber modes are discussed in Section 2.2, where it is shown that a step-index fiber supports a single mode if  $V < 2.405$ . Optical fibers designed to satisfy this condition are called single-mode fibers. The main difference between the single-mode and multimode fibers is the core size. The core radius  $a$  is typically  $25 \mu\text{m}$  for multimode fibers. However, single-mode fibers with  $\Delta \approx 0.003$  require  $a$  to be  $< 5 \mu\text{m}$ . The numerical value of the outer radius  $b$  is less critical as long as it is large enough to confine the fiber modes entirely. A standard value of  $b = 62.5 \mu\text{m}$  is commonly used for both single-mode and multimode fibers. Since nonlinear effects are mostly studied using single-mode fibers, the term optical fiber in this text refers to single-mode fibers (unless noted otherwise).

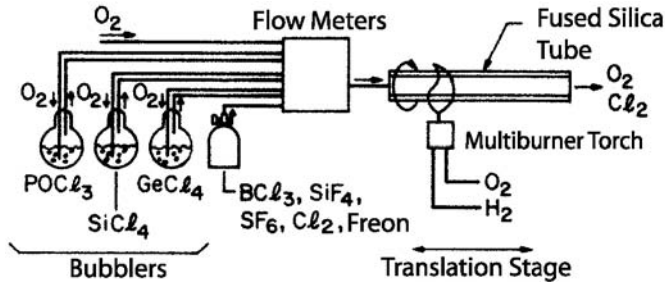


**Figure 1.2:** Schematic diagram of the MCVD process commonly used for fiber fabrication. (After Ref. [70]; ©1985 Elsevier.)

### 1.2.1 Material and Fabrication

The material of choice for low-loss optical fibers is pure silica glass synthesized by fusing  $\text{SiO}_2$  molecules. The refractive-index difference between the core and the cladding is realized by the selective use of dopants during the fabrication process. Dopants such as  $\text{GeO}_2$  and  $\text{P}_2\text{O}_5$  increase the refractive index of pure silica and are suitable for the core, while materials such as boron and fluorine are used for the cladding because they decrease the refractive index of silica. Additional dopants can be used depending on specific applications. For example, to make fiber amplifiers and lasers, the core of silica fibers is codoped with rare-earth ions using dopants such as  $\text{ErCl}_3$  and  $\text{Nd}_2\text{O}_3$ .

The fabrication of optical fibers involves two stages [70]. In the first stage, a vapor-deposition method is used to make a cylindrical preform with the desired refractive-index profile and the relative core-cladding dimensions. A typical preform is 1-m long with a 2-cm diameter. In the second stage, the preform is drawn into a fiber using a precision-feed mechanism that feeds it into a furnace at a proper speed. During this process, the relative core-cladding dimensions are preserved. Both stages, preform fabrication and fiber drawing, involve sophisticated technology to ensure the uniformity of the core size and the index profile [70]–[72].

Several methods can be used for making a preform. The three commonly used methods are modified chemical vapor deposition (MCVD), outside vapor deposition, and vapor-phase axial deposition. Figure 1.2 shows a schematic diagram of the MCVD process. In this process, successive layers of  $\text{SiO}_2$  are deposited on the inside of a fused silica tube by mixing the vapors of  $\text{SiCl}_4$  and  $\text{O}_2$  at a temperature of  $\approx 1800^\circ\text{C}$ . To ensure uniformity, the multiburner torch is moved back and forth across the tube length. The refractive index of the cladding layers is controlled by adding fluorine to the tube. When a sufficient cladding thickness has been deposited with multiple passes of the torch, the vapors of  $\text{GeCl}_4$  or  $\text{POCl}_3$  are added to the vapor mixture to form the core. When all layers have been deposited, the torch temperature is raised to collapse the tube into a solid rod known as the preform.

This description is extremely brief and is intended to provide a general idea. The fabrication of optical fibers requires attention to a large number of technological details. The interested reader is referred to the extensive literature on this subject [70]–[72].

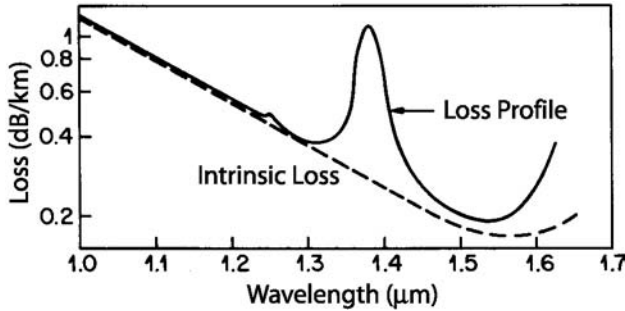


**Figure 1.3:** Measured loss spectrum of a single-mode silica fiber. Dashed curve shows the contribution resulting from Rayleigh scattering. (After Ref. [70]; ©1985 Elsevier.)

### 1.2.2 Fiber Losses

An important fiber parameter provides a measure of power loss during transmission of optical signals inside the fiber. If  $P_0$  is the power launched at the input of a fiber of length  $L$ , the transmitted power  $P_T$  is given by

$$P_T = P_0 \exp(-\alpha L), \quad (1.2.3)$$

where the *attenuation constant*  $\alpha$  is a measure of total fiber losses from all sources. It is customary to express  $\alpha$  in units of dB/km using the relation (see Appendix A for an explanation of decibel units)

$$\alpha_{\text{dB}} = -\frac{10}{L} \log \left( \frac{P_T}{P_0} \right) = 4.343\alpha, \quad (1.2.4)$$

where Eq. (1.2.3) was used to relate  $\alpha_{\text{dB}}$  and  $\alpha$ .

As one may expect, fiber losses depend on the wavelength of light. Figure 1.3 shows the loss spectrum of a silica fiber made by the MCVD process [70]. This fiber exhibits a minimum loss of about 0.2 dB/km near 1.55  $\mu\text{m}$ . Losses are considerably higher at shorter wavelengths, reaching a level of a few dB/km in the visible region. Note, however, that even a 10-dB/km loss corresponds to an attenuation constant of only  $\alpha \approx 2 \times 10^{-5} \text{ cm}^{-1}$ , an incredibly low value compared to that of most other materials.

Several factors contribute to the loss spectrum of Figure 1.3, with material absorption and *Rayleigh scattering* contributing dominantly. Silica glass has electronic resonances in the ultraviolet region, and vibrational resonances in the far-infrared region beyond 2  $\mu\text{m}$ , but it absorbs little light in the wavelength region extending from 0.5 to 2  $\mu\text{m}$ . However, even a relatively small amount of impurities can lead to significant absorption in that wavelength window. From a practical point of view, the most important impurity affecting fiber loss is the OH ion, which has a fundamental vibrational absorption peak at  $\approx 2.73 \mu\text{m}$ . The overtones of this OH-absorption peak are responsible for the dominant peak seen in Figure 1.3 near 1.4  $\mu\text{m}$  and a smaller peak near 1.23  $\mu\text{m}$ . Special precautions are taken during the fiber-fabrication process

to ensure an OH-ion level of less than one part in one hundred million [70]. In state-of-the-art fibers, the peak near  $1.4 \mu\text{m}$  can be reduced to below the 0.5-dB level. It virtually disappears in the so-called “dry” fibers [73]. Such fibers with low losses in the entire  $1.3\text{--}1.6 \mu\text{m}$  spectral region are useful for fiber-optic communications and were available commercially by the year 2000.

Rayleigh scattering is a fundamental loss mechanism arising from density fluctuations frozen into the fused silica during manufacture. Resulting local fluctuations in the refractive index scatter light in all directions. The Rayleigh-scattering loss varies as  $\lambda^{-4}$  and is dominant at short wavelengths. As this loss is intrinsic to the fiber, it sets the ultimate limit on fiber loss. The intrinsic loss level (shown by a dashed line in Figure 1.3) is estimated to be (in dB/km)

$$\alpha_R = C_R/\lambda^4, \quad (1.2.5)$$

where the constant  $C_R$  is in the range  $0.7\text{--}0.9 \text{ dB}/(\text{km}\cdot\mu\text{m}^4)$  depending on the constituents of the fiber core. As  $\alpha_R$  is in the range of  $0.12\text{--}0.15 \text{ dB}/\text{km}$  near  $\lambda = 1.55 \mu\text{m}$ , losses in silica fibers are dominated by Rayleigh scattering. In some glasses,  $\alpha_R$  can be reduced to a level near  $0.05 \text{ dB}/\text{km}$  [74]. Such glasses may be useful for fabricating ultralow-loss fibers.

Among other factors that may contribute to losses are bending of fiber and scattering of light at the core-cladding interface [67]. Modern fibers exhibit a loss of  $\approx 0.2 \text{ dB}/\text{km}$  near  $1.55 \mu\text{m}$ . Total loss of fiber cables used in optical communication systems is slightly larger because of splice and cabling losses.

### 1.2.3 Chromatic Dispersion

When an electromagnetic wave interacts with the bound electrons of a dielectric, the medium response, in general, depends on the optical frequency  $\omega$ . This property, referred to as chromatic dispersion, manifests through the frequency dependence of the refractive index  $n(\omega)$ . On a fundamental level, the origin of chromatic dispersion is related to the characteristic resonance frequencies at which the medium absorbs the electromagnetic radiation through oscillations of bound electrons. Far from the medium resonances, the refractive index is well approximated by the *Sellmeier equation* [67]

$$n^2(\omega) = 1 + \sum_{j=1}^m \frac{B_j \omega_j^2}{\omega_j^2 - \omega^2}, \quad (1.2.6)$$

where  $\omega_j$  is the resonance frequency and  $B_j$  is the strength of  $j$ th resonance. The sum in Eq. (1.2.6) extends over all material resonances that contribute to the frequency range of interest. In the case of optical fibers, the parameters  $B_j$  and  $\omega_j$  are obtained experimentally by fitting the measured dispersion curves [75] to Eq. (1.2.6) with  $m = 3$  and depend on the core constituents [69]. For bulk-fused silica, these parameters are found to be [76]  $B_1 = 0.6961663$ ,  $B_2 = 0.4079426$ ,  $B_3 = 0.8974794$ ,  $\lambda_1 = 0.0684043 \mu\text{m}$ ,  $\lambda_2 = 0.1162414 \mu\text{m}$ , and  $\lambda_3 = 9.896161 \mu\text{m}$ , where  $\lambda_j = 2\pi c/\omega_j$  and  $c$  is the speed of light in vacuum. Figure 1.4 displays how  $n$  varies with wavelength for fused silica. As seen there,  $n$  has a value of about 1.46 in the visible region, and this value decreases by 1% in the wavelength region near  $1.5 \mu\text{m}$ .



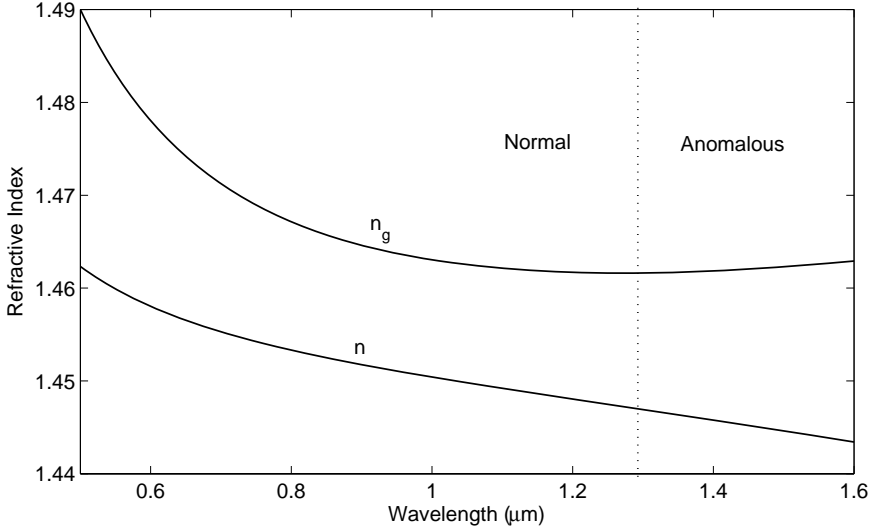


**Figure 1.4:** Variation of refractive index  $n$  and group index  $n_g$  with wavelength for fused silica.

Fiber dispersion plays a critical role in propagation of short optical pulses because different spectral components associated with the pulse travel at different speeds given by  $c/n(\omega)$ . Even when the nonlinear effects are not important, dispersion-induced pulse broadening can be detrimental for optical communication systems. In the nonlinear regime, the combination of dispersion and nonlinearity can result in a qualitatively different behavior, as discussed in later chapters. Mathematically, the effects of fiber dispersion are accounted for by expanding the mode-propagation constant  $\beta$  in a Taylor series about the frequency  $\omega_0$  at which the pulse spectrum is centered:

$$\beta(\omega) = n(\omega) \frac{\omega}{c} = \beta_0 + \beta_1(\omega - \omega_0) + \frac{1}{2}\beta_2(\omega - \omega_0)^2 + \dots, \quad (1.2.7)$$

where

$$\beta_m = \left( \frac{d^m \beta}{d\omega^m} \right)_{\omega=\omega_0} \quad (m = 0, 1, 2, \dots). \quad (1.2.8)$$

The parameters  $\beta_1$  and  $\beta_2$  are related to the refractive index  $n(\omega)$  and its derivatives through the relations

$$\beta_1 = \frac{1}{v_g} = \frac{n_g}{c} = \frac{1}{c} \left( n + \omega \frac{dn}{d\omega} \right), \quad (1.2.9)$$

$$\beta_2 = \frac{1}{c} \left( 2 \frac{dn}{d\omega} + \omega \frac{d^2 n}{d\omega^2} \right), \quad (1.2.10)$$

where  $n_g$  is the group index and  $v_g$  is the group velocity. Figure 1.4 shows the group index  $n_g$  changes with wavelength for fused silica. The group velocity can be found using  $\beta_1 = c/n_g$ . Physically speaking, the envelope of an optical pulse moves at the

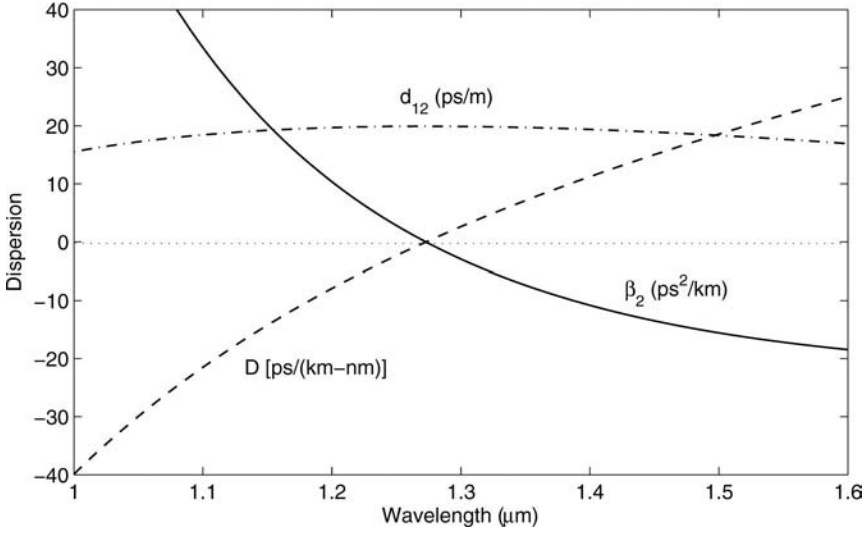


**Figure 1.5:** Variation of  $\beta_2$ ,  $D$ , and  $d_{12}$  with wavelength for fused silica. Both  $\beta_2$  and  $D$  vanish at the zero-dispersion wavelength occurring near  $1.27 \mu\text{m}$ .

group velocity, while the parameter  $\beta_2$  represents dispersion of the group velocity and is responsible for pulse broadening. This phenomenon is known as the *group-velocity dispersion* (GVD), and  $\beta_2$  is the GVD parameter. The dispersion parameter  $D$ , defined as  $d\beta_1/d\lambda$ , is also used in practice. It is related to  $\beta_2$  and  $n$  as

$$D = \frac{d\beta_1}{d\lambda} = -\frac{2\pi c}{\lambda^2} \beta_2 = -\frac{\lambda}{c} \frac{d^2 n}{d\lambda^2}. \quad (1.2.11)$$

Figure 1.5 shows how  $\beta_2$  and  $D$  vary with wavelength  $\lambda$  for fused silica using Eqs. (1.2.6) and (1.2.10). The most notable feature is that both  $\beta_2$  and  $D$  vanish at a wavelength of about  $1.27 \mu\text{m}$  and change sign for longer wavelengths. This wavelength is referred to as the *zero-dispersion wavelength* and is denoted as  $\lambda_D$ . However, the dispersive effects do not disappear completely at  $\lambda = \lambda_D$ . Pulse propagation near this wavelength requires inclusion of the cubic term in Eq. (1.2.7). The coefficient  $\beta_3$  appearing in that term is called the *third-order dispersion* (TOD) parameter. Higher-order dispersive effects can distort ultrashort optical pulses both in the linear [67] and non-linear regimes [77]. Their inclusion is necessary for ultrashort optical pulses, or when the input wavelength  $\lambda$  approaches  $\lambda_D$  to within a few nanometers.

The curves shown in Figures 1.4 and 1.5 are for bulk-fused silica. The dispersive behavior of actual glass fibers deviates from that shown in these figures for the following two reasons. First, the fiber core may have small amounts of dopants such as  $\text{GeO}_2$  and  $\text{P}_2\text{O}_5$ . Equation (1.2.6) in that case should be used with parameters appropriate to the amount of doping levels [69]. Second, because of dielectric waveguiding, the effective mode index is slightly lower than the material index  $n(\omega)$  of the core, reduction itself being  $\omega$  dependent [67]–[69]. This results in a waveguide contribution that

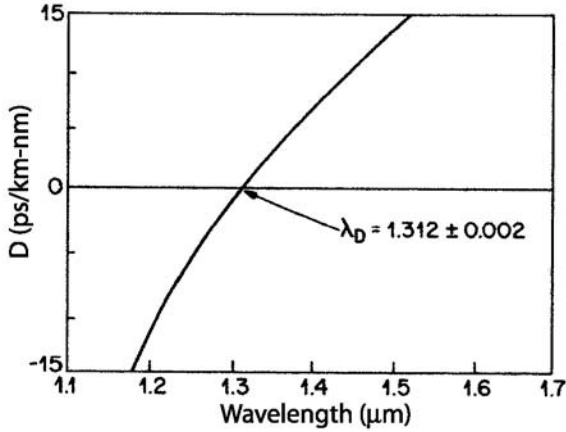


**Figure 1.6:** Measured variation of dispersion parameter  $D$  with wavelength for a single-mode fiber. (After Ref. [70]; ©1985 Elsevier.)

must be added to the material contribution to obtain the total dispersion. Generally, the waveguide contribution to  $\beta_2$  is relatively small except near the zero-dispersion wavelength  $\lambda_D$  where the two become comparable. The main effect of the waveguide contribution is to shift  $\lambda_D$  slightly toward longer wavelengths;  $\lambda_D \approx 1.31 \mu\text{m}$  for standard fibers. Figure 1.6 shows the measured total dispersion of a single-mode fiber [70]. The quantity plotted is the dispersion parameter  $D$  related to  $\beta_2$  by the relation given in Eq. (1.2.11).

An interesting feature of the waveguide dispersion is that its contribution to  $D$  (or  $\beta_2$ ) depends on fiber-design parameters such as core radius  $a$  and core-cladding index difference  $\Delta$ . This feature can be used to shift the zero-dispersion wavelength  $\lambda_D$  in the vicinity of  $1.55 \mu\text{m}$  where the fiber loss is minimum. Such *dispersion-shifted* fibers [78] have found applications in optical communication systems. They are available commercially and are known by names such as TrueWave (Lucent), LEAF (Corning), and TeraLight (Alcatel), depending on at what wavelength  $D$  becomes zero in the  $1.5 \mu\text{m}$  spectral region. The fibers in which GVD is shifted to the wavelength region beyond  $1.6 \mu\text{m}$  exhibit a large positive value of  $\beta_2$ . They are called *dispersion-compensating fibers* (DCFs). The slope of the curve in Figure 1.6 (called the *dispersion slope*) is related to the TOD parameter  $\beta_3$ . Fibers with reduced slope have been developed in recent years for wavelength-division-multiplexing (WDM) applications.

It is possible to design *dispersion-flattened* optical fibers having low dispersion over a relatively large wavelength range of  $1.3$ – $1.6 \mu\text{m}$ . This is achieved by using multiple cladding layers. Figure 1.7 shows the measured dispersion spectra for two such multiple-clad fibers having two (double-clad) and four (quadruple-clad) cladding layers around the core applications. For comparison, dispersion of a single-clad fiber is also shown by a dashed line. The quadruply clad fiber has low dispersion ( $|D| \sim 1 \text{ ps/km-nm}$ ) over a wide wavelength range extending from  $1.25$  to  $1.65 \mu\text{m}$ . Waveguide dispersion can also be used to make fibers for which  $D$  varies along the fiber length.

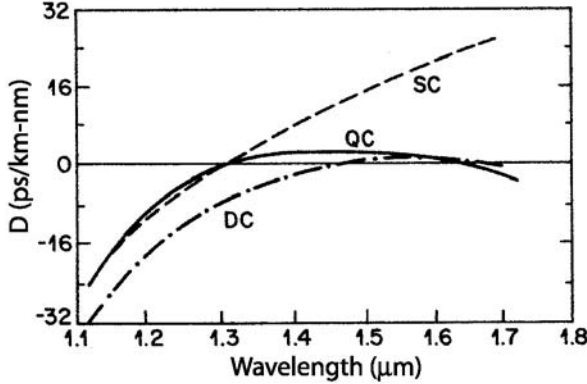


**Figure 1.7:** Variation of dispersion parameter  $D$  with wavelength for three kinds of fibers. Labels SC, DC, and QC stand for single-clad, double-clad, and quadruple-clad fibers, respectively. (After Ref. [79]; ©1982 IEE.)

An example is provided by *dispersion-decreasing* fibers made by tapering the core diameter along the fiber length [80].

Nonlinear effects in optical fibers can manifest qualitatively different behaviors depending on the sign of the GVD parameter. For wavelengths such that  $\lambda < \lambda_D$ , the fiber is said to exhibit *normal dispersion* as  $\beta_2 > 0$  (see Figure 1.5). In the normal-dispersion regime, high-frequency (blue-shifted) components of an optical pulse travel slower than low-frequency (red-shifted) components of the same pulse. By contrast, the opposite occurs in the *anomalous dispersion* regime in which  $\beta_2 < 0$ . As seen in Figure 1.5, silica fibers exhibit anomalous dispersion when the light wavelength exceeds the zero-dispersion wavelength ( $\lambda > \lambda_D$ ). The anomalous-dispersion regime is of considerable interest for the study of nonlinear effects because it is in this regime that optical fibers support solitons through a balance between the dispersive and nonlinear effects.

An important feature of chromatic dispersion is that pulses at different wavelengths propagate at different speeds inside a fiber because of a mismatch in their group velocities. This feature leads to a walk-off effect that plays an important role in the description of the nonlinear phenomena involving two or more closely spaced optical pulses. More specifically, the nonlinear interaction between two optical pulses ceases to occur when the faster moving pulse completely walks through the slower moving pulse. This feature is governed by the *walk-off parameter*  $d_{12}$  defined as

$$d_{12} = \beta_1(\lambda_1) - \beta_1(\lambda_2) = v_g^{-1}(\lambda_1) - v_g^{-1}(\lambda_2), \quad (1.2.12)$$

where  $\lambda_1$  and  $\lambda_2$  are the center wavelengths of two pulses and  $\beta_1$  at these wavelengths is evaluated using Eq. (1.2.9). For pulses of width  $T_0$ , one can define the walk-off length  $L_W$  by the relation

$$L_W = T_0 / |d_{12}|. \quad (1.2.13)$$

Figure 1.5 shows variation of  $d_{12}$  with  $\lambda_1$  for fused silica using Eq. (1.2.12) with  $\lambda_2 = 0.8 \mu\text{m}$ . In the normal-dispersion regime ( $\beta_2 > 0$ ), a longer-wavelength pulse travels